Supporting Information for "Dominant terms in the freshwater and heat budgets of the subpolar North Atlantic Ocean and Nordic Seas from 1992 to 2015"

Jan-Erik Tesdal[1], Thomas W. N. Haine[2]

[1]Lamont-Doherty Earth Observatory, Columbia University, Palisades, New York, USA

[2]Earth and Planetary Sciences, The Johns Hopkins University, Baltimore, Maryland, USA

Contents of this file

Text S1.

The supplemental material includes additional results supporting the main findings of the article. In particular, Figures S2, S6, and S7 include budget results for salinity, which clarifies the consistency between liquid freshwater content and salinity in our results .

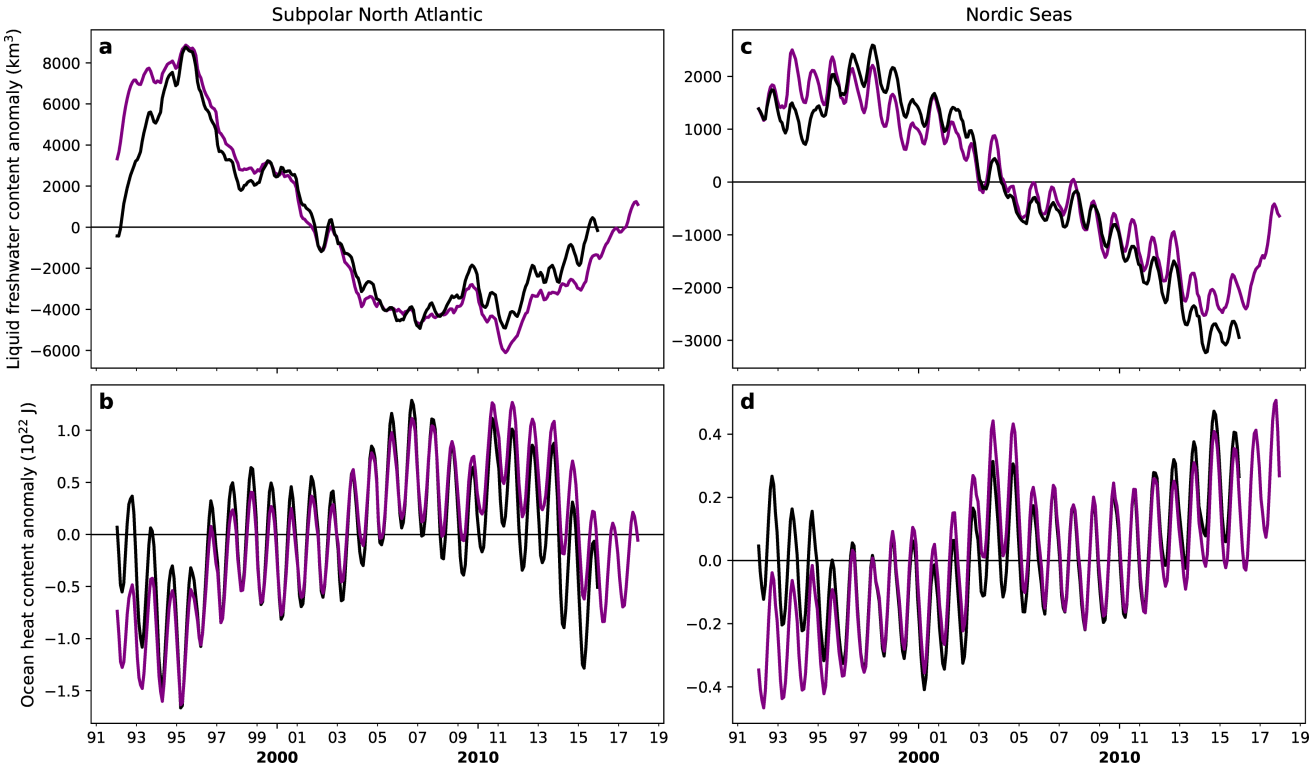

Figure S1. Liquid freshwater and heat content anomalies from ECCOv4 over the (a,b) subpolar North Atlantic and (c,d) Nordic Seas. For comparison, estimates are included for spatial definition as in Figure 1 using Release 3 (1992-2015, black line) and as defined in Figure 3a with Release 4 (1992-2017, purple line). Note the different y scales for the subpolar North Atlantic (a,b) and Nordic Seas (c,d).

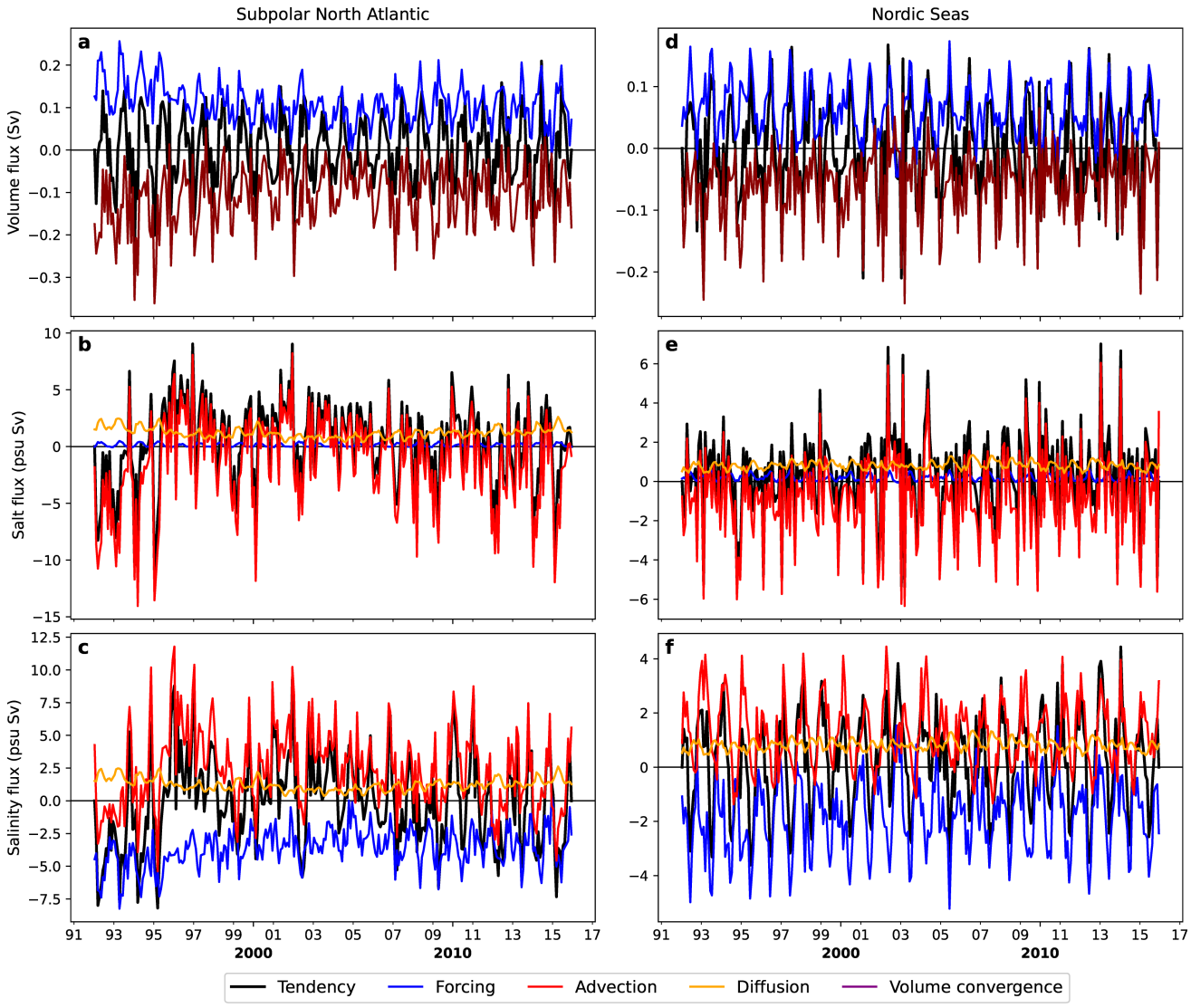

Figure S2. Monthly time series of volume, salt and salinity fluxes of the (a-c) subpolar North Atlantic and (d-f) Nordic Seas, including total tendency and individual components for surface forcing, advection, and diffusion. Note the different y scales for the subpolar North Atlantic (a,b) and Nordic Seas (c,d).

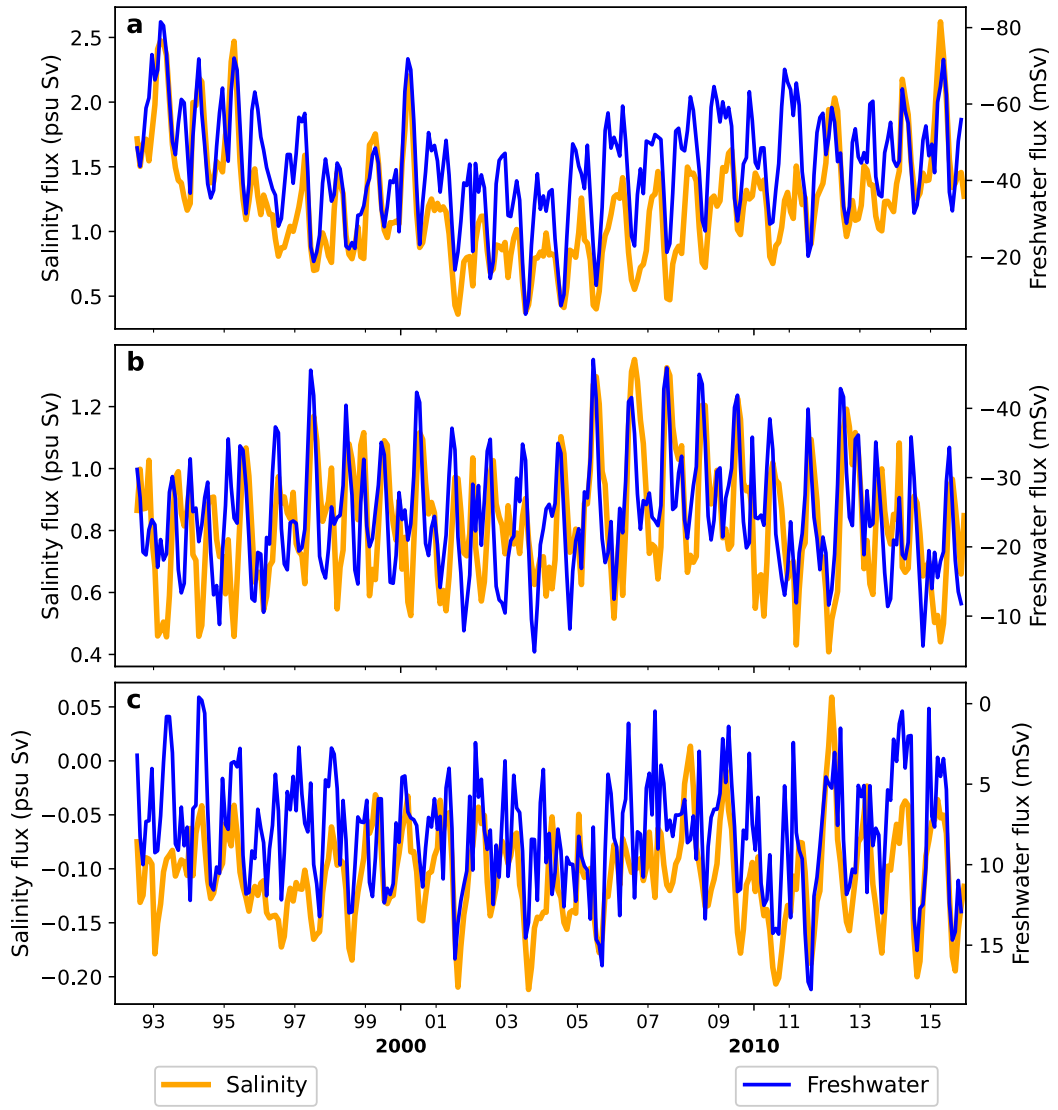

Figure S3. Comparison of diffusive flux convergence between salinity and freshwater for the (a) subpolar North Atlantic, (b) Nordic Seas and (c) Labrador Sea.

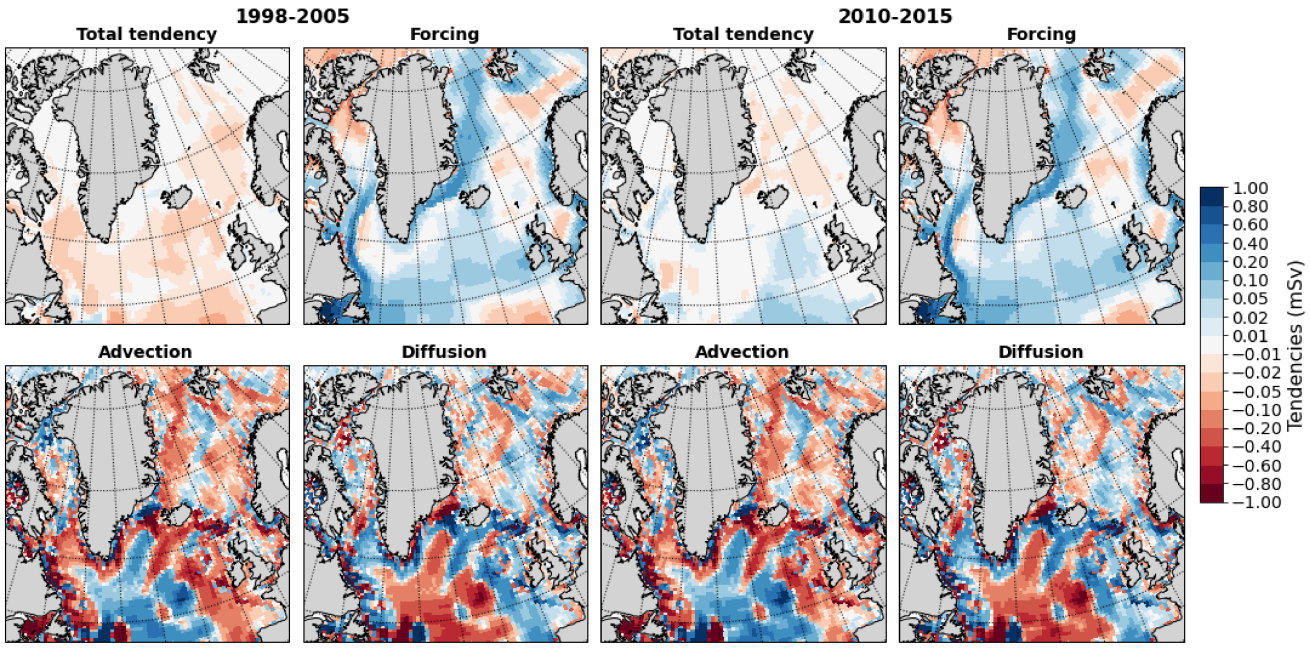

Figure S4. Spatial distributions of means for each major term in the ECCOv4 freshwater budget for the North Atlantic over 1998-2005 and 2010-2015.

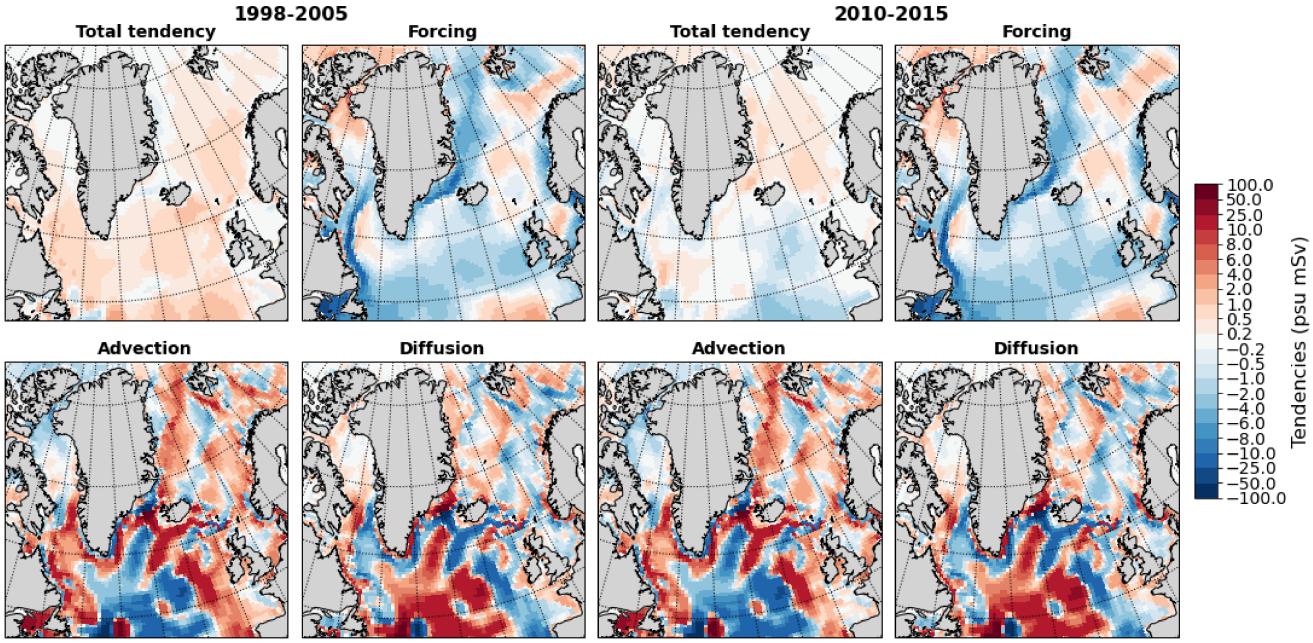

Figure S5. Spatial distributions of means for each major term in the ECCOv4 salinity budget for the North Atlantic over 1998-2005 and 2010-2015.

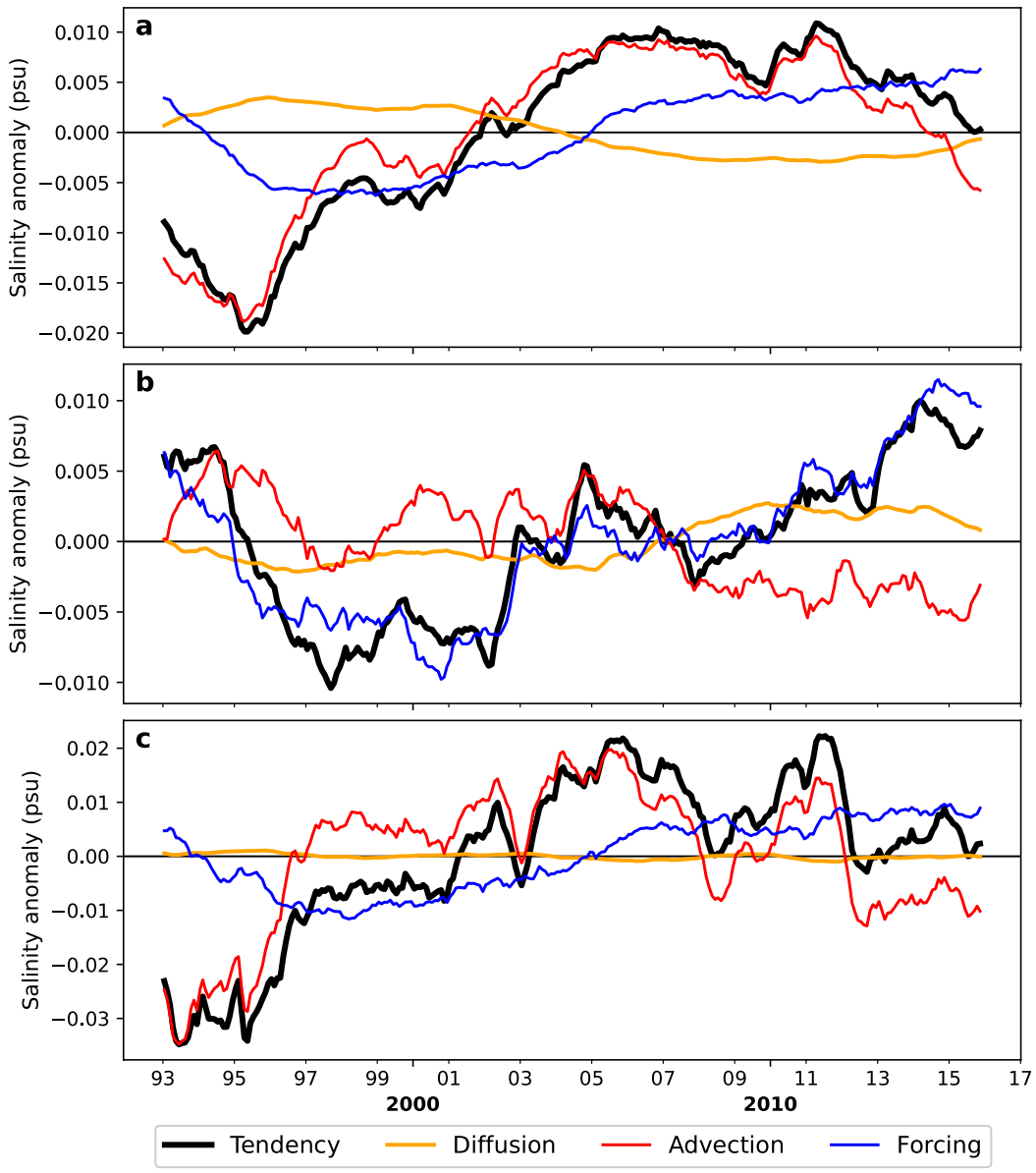

Figure S6. Integrated monthly time series of salinity anomaly for the (a) subpolar North Atlantic, (b) Nordic Seas and (c) Labrador Sea, including total tendency and individual components for surface forcing, advection, and diffusion.

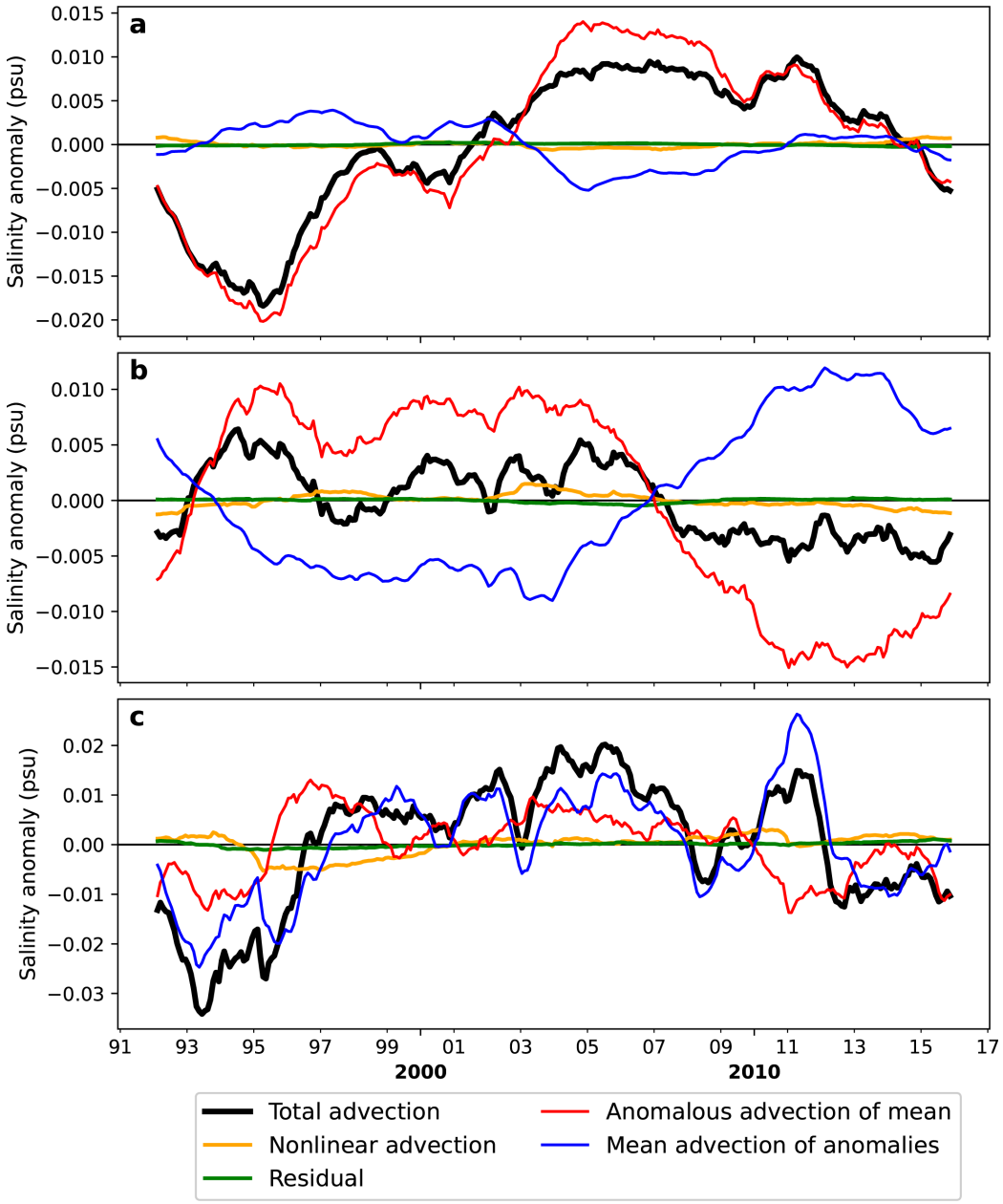

Figure S7. Decomposition of advective convergence of salinity anomaly into contributions from anomalous advection of mean, mean advection of anomalies, nonlinear advection and residual for the (a) subpolar North Atlantic, (b) Nordic Seas and (c) Labrador Sea. Note the different y scales for the subpolar North Atlantic (a,b) and Nordic Seas (c,d).

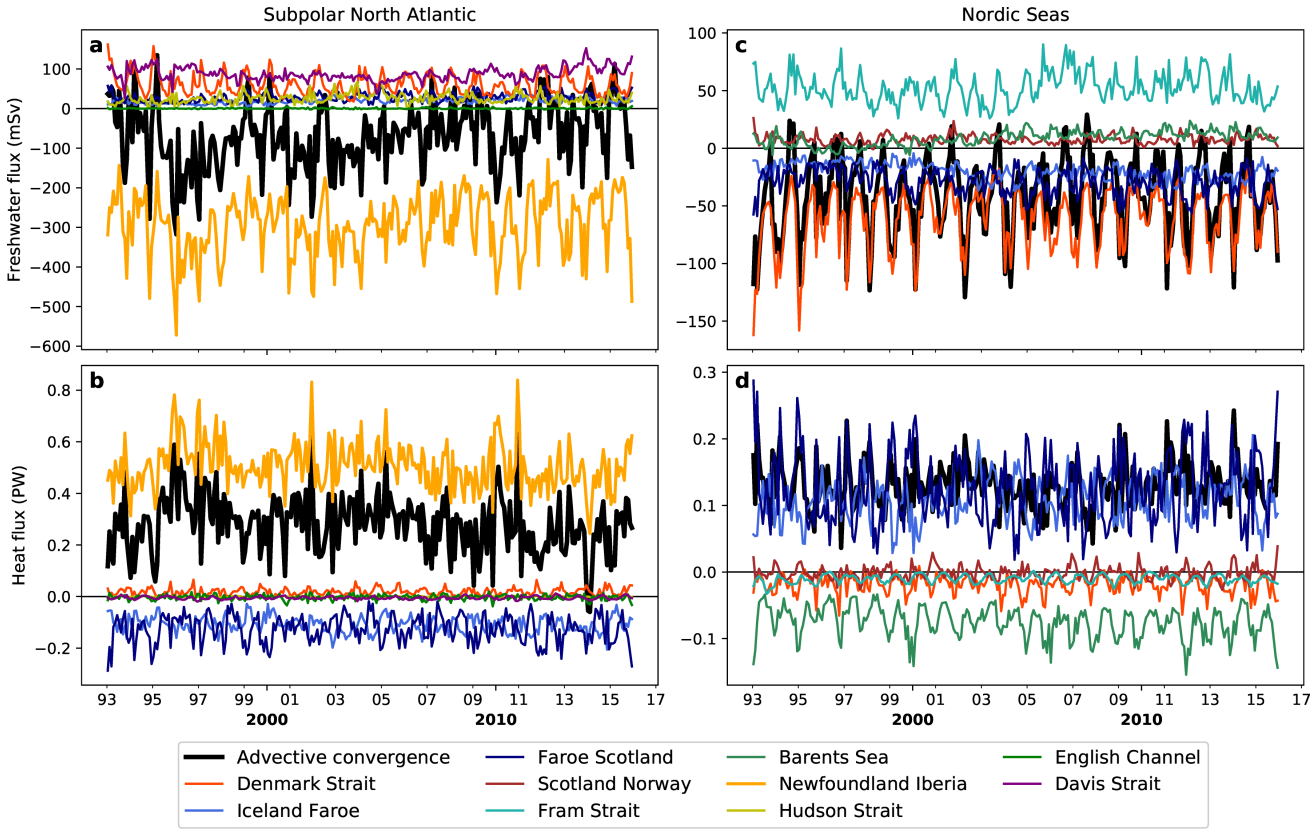

Figure S8. Total advective convergence and boundary fluxes into the (a,b) subpolar North Atlantic and (c,d) Nordic Seas for (a,c) freshwater and (b,d) heat content. Note the different y scales for the subpolar North Atlantic (a,b) and Nordic Seas (c,d).

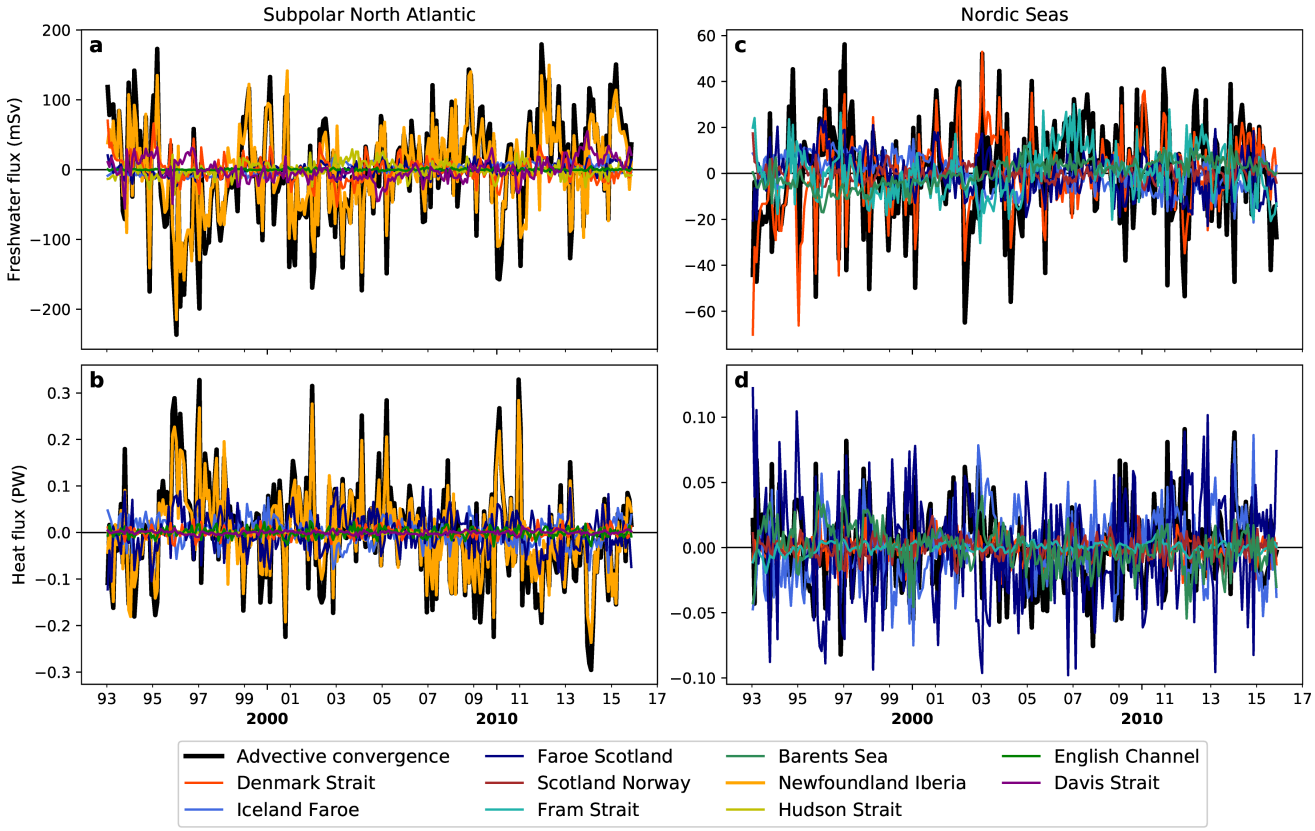

Figure S9. Seasonal anomalies of advective convergence and boundary fluxes into the (a,b) subpolar North Atlantic and (c,d) Nordic Seas for (a,c) freshwater and (b,d) heat content. Note the different y scales for the subpolar North Atlantic (a,b) and Nordic Seas (c,d).

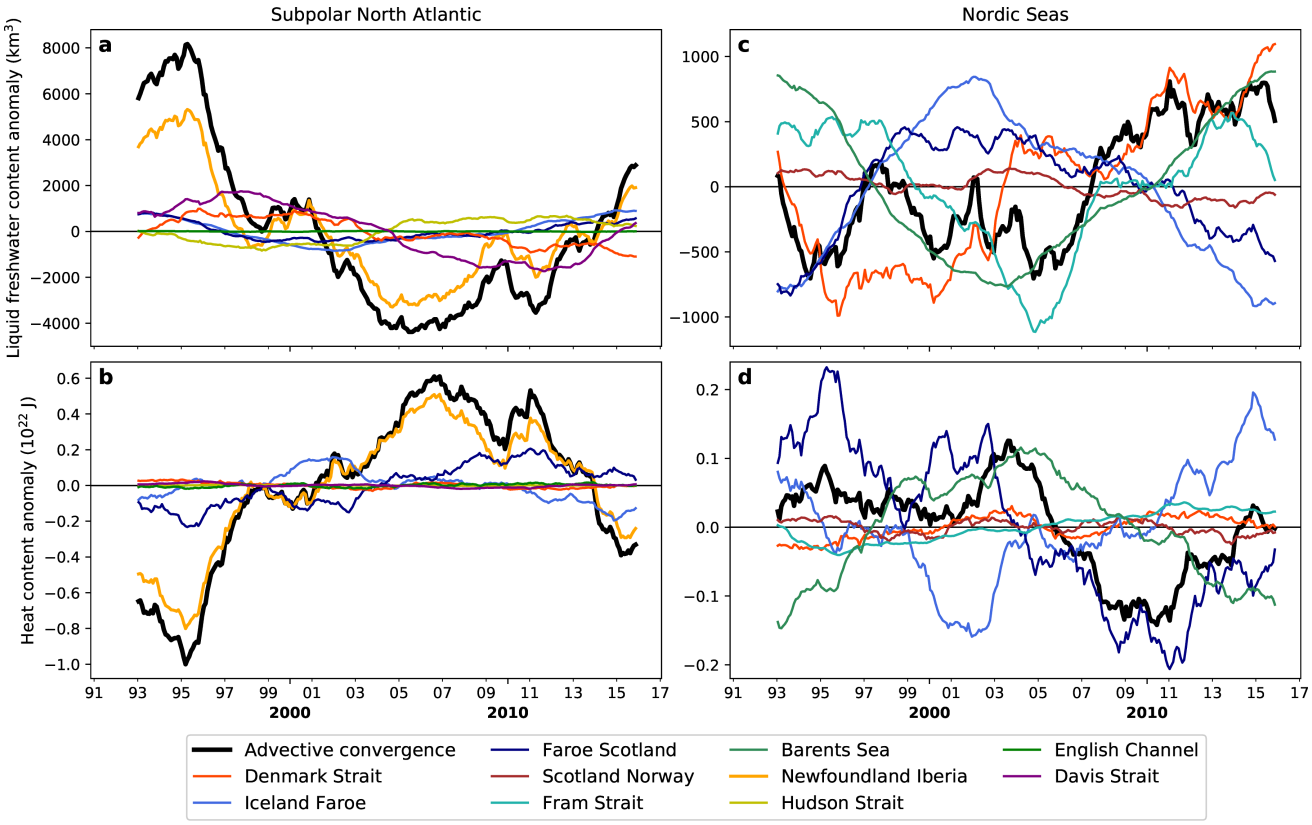

Figure S10. Integrated time series showing the total advective convergence and the contribution of each boundary flux into the (a,b) subpolar North Atlantic and (c,d) Nordic Seas for (a,c) freshwater and (b,d) heat content. Note the different y scales for the subpolar North Atlantic (a,b) and Nordic Seas (c,d).

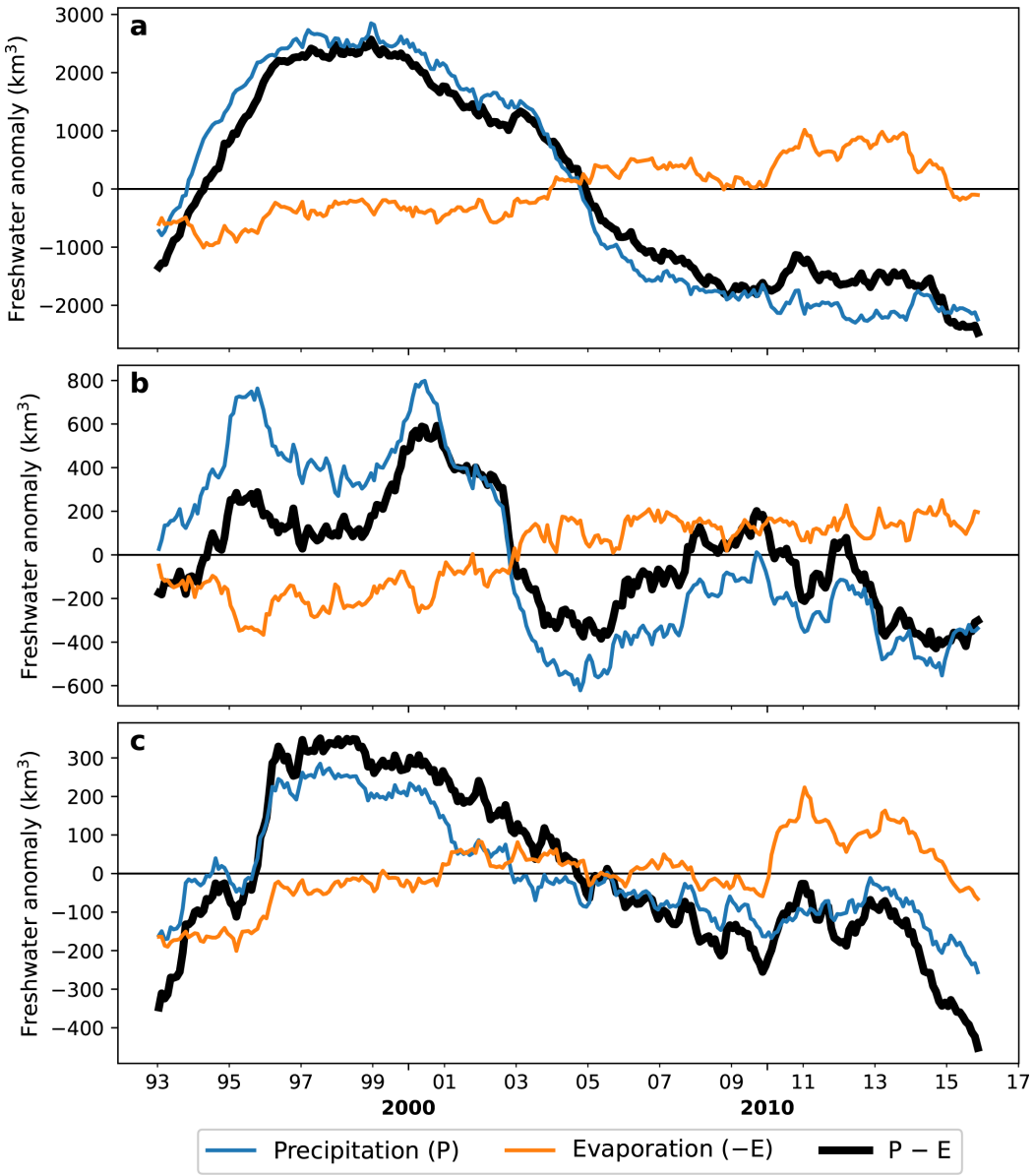

Figure S11. Decomposition of atmospheric freshwater flux into precipitation and evaporation for the (a) subpolar North Atlantic, (b) Nordic Seas and (c) Labrador Sea.

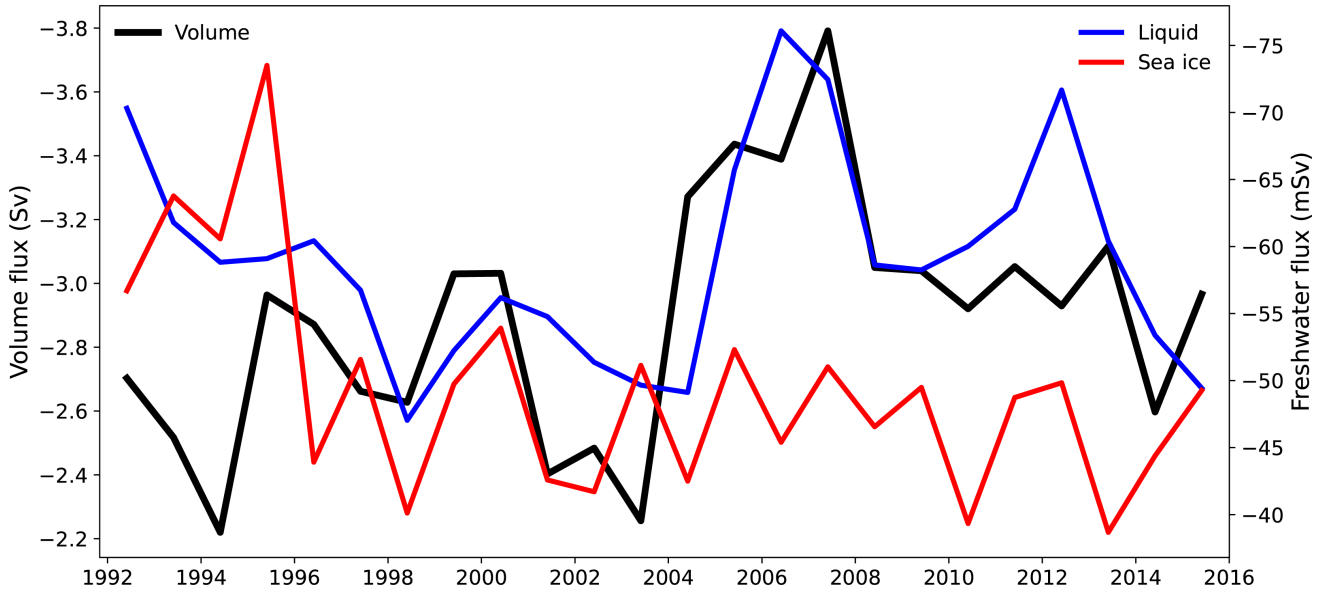

Figure S12. Annual means of volume and freshwater fluxes through the Fram Strait. Freshwater fluxes are shown for liquid freshwater and sea ice.

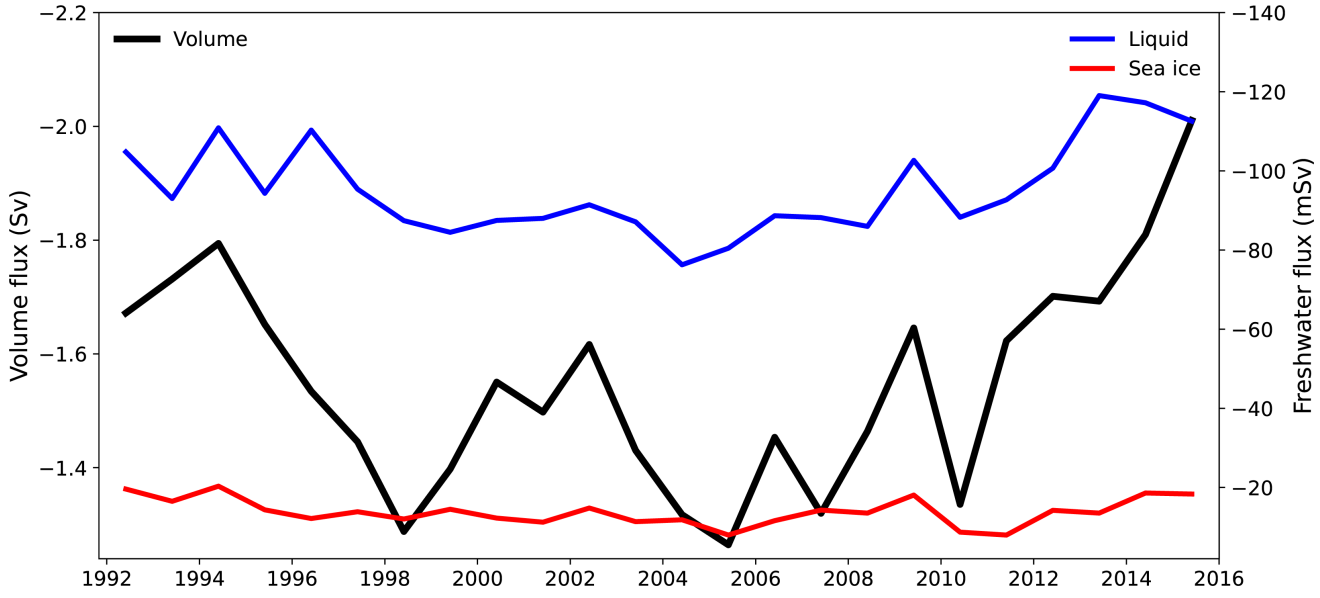

Figure S13. Annual means of volume and freshwater fluxes through the Davis Strait. Freshwater fluxes are shown for liquid freshwater and sea ice.

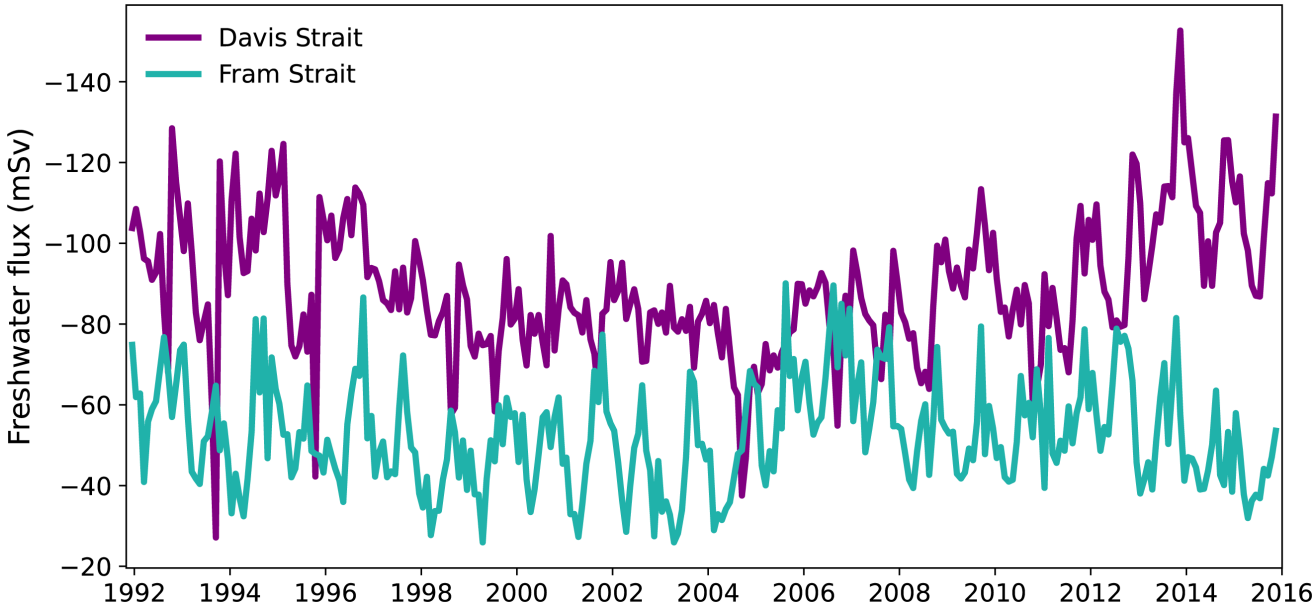

Figure S14. Comparison of monthly mean freshwater fluxes through the Davis Strait and Fram Strait. Freshwater fluxes are calculated using $S_{ref} = 35\,g\,kg^{-1}$.

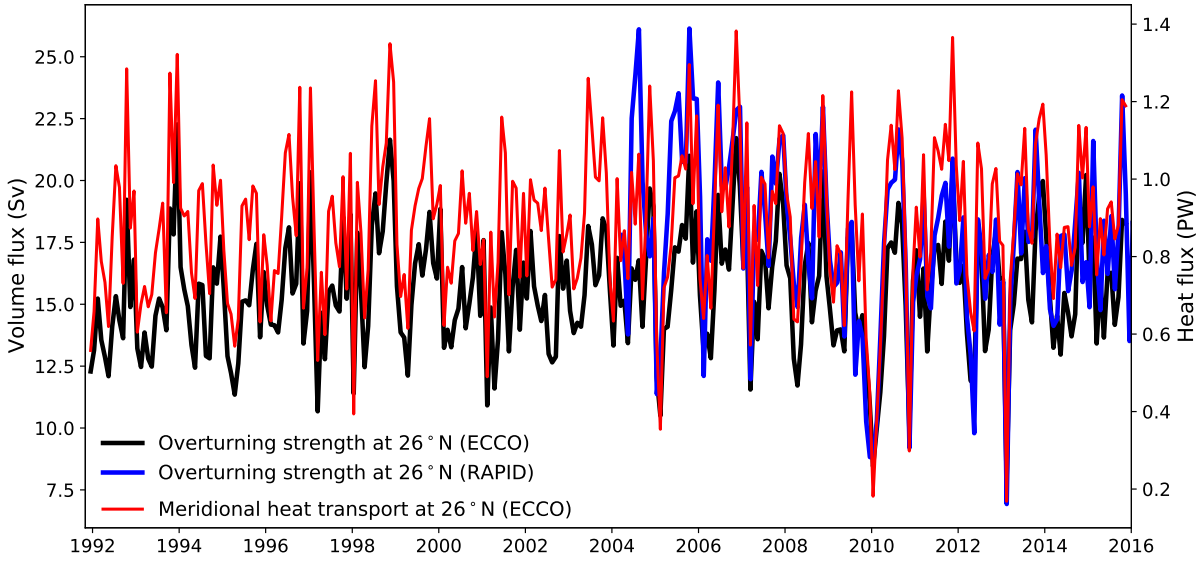

Figure S15. Comparison of AMOC strength (black) and meridional heat flux (red) estimate from ECCOv4 plotted with AMOC strength from RAPID (blue) at 26°N.

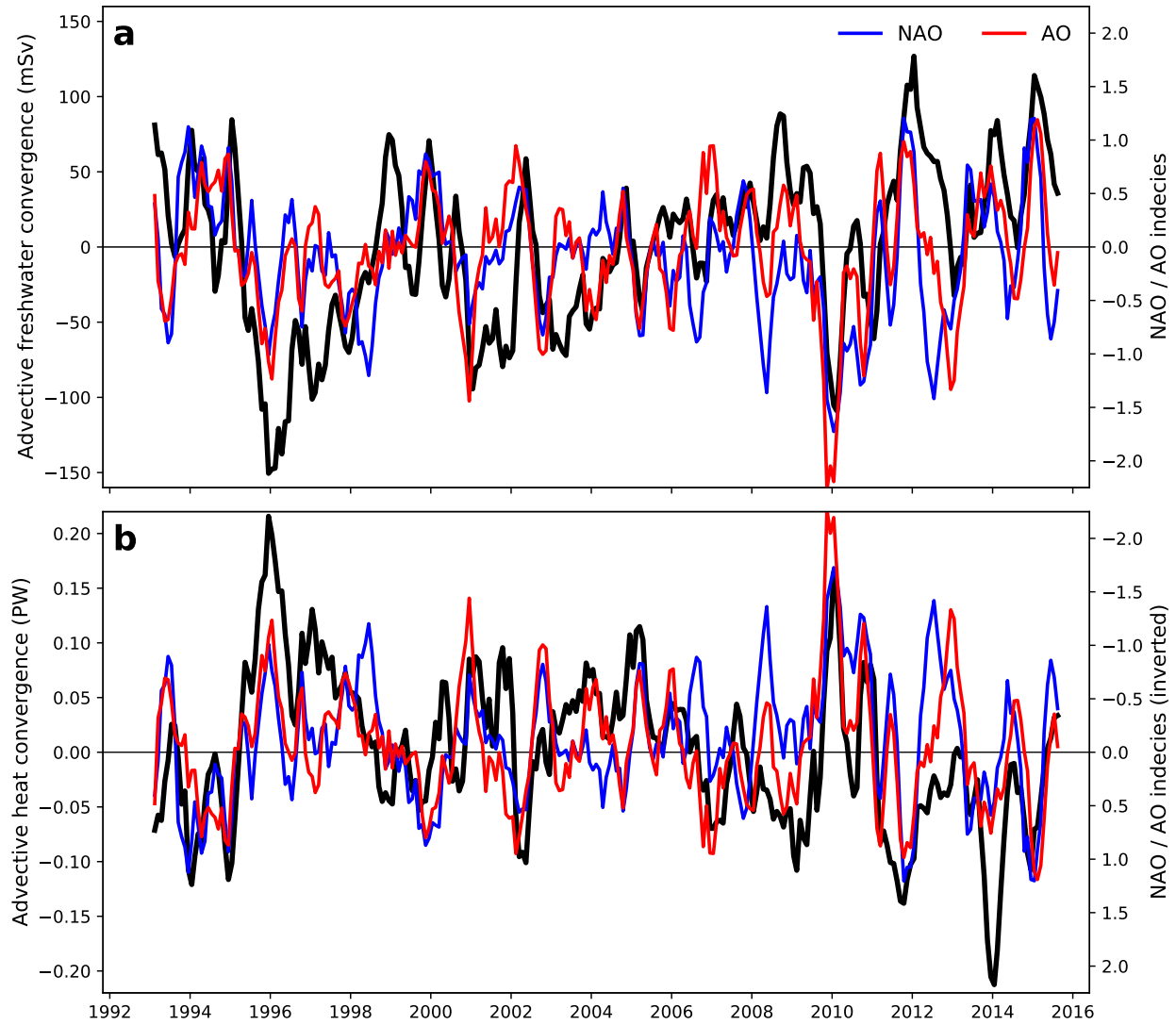

Figure S16. Anomalous advective (a) freshwater and (b) heat convergence in the SPNA (black) plotted with time series of NAO (blue) and AO climate index (red). Note that y axis for NAO/AO is inverted in panel b.

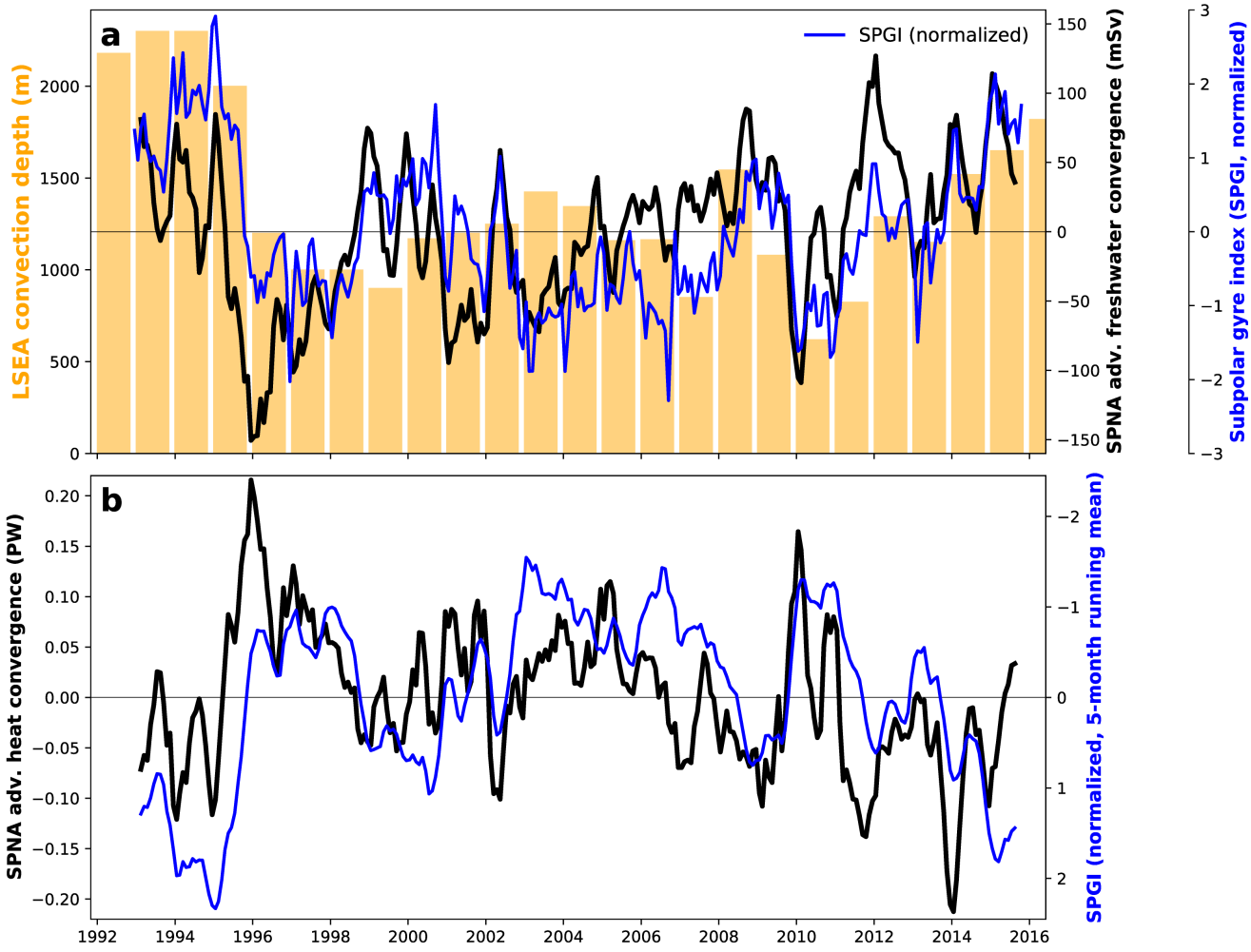

Figure S17. (a) Winter convective depth in the Labrador Sea (LSEA) plotted with anomalous advective freshwater convergence and monthly time series of SPGI (blue). (b) Anomalous heat convergence in the SPNA (black) plotted with 5-month running mean of SPGI (blue). SPGI has been normalized by subtracting its mean and dividing it by its standard deviation. Note that y axis for SPGI is inverted in panel b.